Proc. Natl. Acad. Sci. USA
Vol. 86, pp. 7937–7941, October 1989
Evolution

Traveling waves of *in vitro* evolving RNA

(selection/reaction–diffusion/capillary/Qβ replicase/fluorescence)

G. J. BAUER, J. S. MCCASKILL†, AND H. OTTEN

Max-Planck-Institut für Biophysikalische Chemie, Nikolausberg am Faßberg, D-3400 Göttingen, Federal Republic of Germany

Communicated by Manfred Eigen, July 17, 1989

ABSTRACT **Populations of short self-replicating RNA variants have been confined to one side of a reaction–diffusion traveling wave front propagating along thin capillary tubes containing the Qβ viral enzyme. The propagation speed is accurately measurable with a magnitude of about 1 μm/sec, and the wave persists for hundreds of generations (of duration less than 1 min). Evolution of RNA occurs in the wavefront, as established by front velocity changes and gel electrophoresis of samples drawn from along the capillary. The high population numbers (≈10^{11}), their well-characterized biochemistry, their short generation time, and the constant conditions make the system ideal for evolution experiments. Growth is monitored continuously by excitation of an added RNA-sensitive fluorescent dye, ethidium bromide. An analytic expression for the front velocity is derived for the multicomponent kinetic scheme that reduces, for a high RNA–enzyme binding constant, to the Fisher form $v = 2\sqrt{\kappa D}$, where D is the diffusion constant of the complex and κ is the low-concentration overall replication rate coefficient. The latter is confirmed as the selective value-determining parameter by numerical solution of a two-species system.**

It is difficult to provide a constant set of conditions for an explosive reaction over long periods. In a chemical traveling wave, constant reaction conditions are maintained in spite of an intrinsic stability in the homogeneous kinetics (1). The stirred flow reactor (2) and serial transfer method (3) represent laboratory techniques for establishing homogeneous constant chemical conditions. Studies in a constant environment are particularly important to an elementary understanding of molecular evolution. In this work we establish that a constant environment for RNA replication can be attained for a thousand generations or more (corresponding to a day-long experiment) in a traveling concentration wave. The usual difficulties of confinement (10^{14} molecules, with the reaction catalyzed by a single molecule) are resolved by the physical seal of a fluid-filled capillary.

The kinetics of *in vitro* RNA replication for the Qβ system is now known in some detail (4–6). Although many questions pertaining to evolution of RNA molecules in this system are open, it is known (6) that there are essentially two distinct phenotypic environments depending on whether the replicase is in excess with respect to RNA templates or not. In the former phase, the growth of RNA is exponential, and in the latter it is linear, attaining a constant rate as a result of enzyme saturation with template. The importance of this distinction is not simply that the selection theory for such a system of many self-replicating molecules has been solved analytically only for the exponential phase (7–10), but rather that it has been shown that in the linear phase coexistence between molecules of differing replication rates occurs (6). It is this fundamental difference that makes it interesting to characterize the type of evolutionary environment presented by a diffusive front growing along a capillary in which both concentration regimes occur. In particular, does selection occur or does the fact that the bulk of RNA molecules is growing in the linear phase lead to coexistence? If the traveling front perpetuates a reaction volume in the exponential phase, then it represents an ideal reactor for testing and developing selection models.

The formation of complexes between RNA template and enzyme makes the kinetics more complicated than that of the single-component Fisher equation (11) for the concentration $u(x, t)$ of a species at position x at time t, replicating at rate $f(u)$ and with diffusion constant D:

$$\frac{\partial u}{\partial t} = D\frac{\partial^2 u}{\partial x^2} + f(u). \qquad [1]$$

The latter, however, provides a simple reference for a multicomponent analysis (see *The Kinetic Model*) and is regained in special cases. If $f'(u)$ is monotonically decreasing with increasing concentrations u, such as with the logistic growth form $f(u) = ku(1 - u/K)$, where k is the replication rate coefficient and K is the maximum concentration of RNA, then the minimum velocity of a traveling concentration wave is (11)

$$v = 2\sqrt{f'(0)D} \qquad [2]$$

and starting from arbitrary step-function initial-concentration profiles, the solution approaches a traveling wave with this minimum velocity (12, 13).

This behavior has been observed in the capillary experiments reported here: after a short period following inoculation with RNA of a capillary containing the Qβ enzyme solution, a front could be observed that sharpened and slowed down to travel at a constant velocity (see Fig. 1 and below). Sharp changes in the front velocity were also observed (Fig. 1) and their evolutive origin was confirmed in later experiments by electrophoretic analysis of the RNA. The remainder of the article concerns the precise experimental, analytic, and numerical characterization of the selection conditions in the traveling wave.

MATERIALS AND METHODS

Purification of Qβ Replicase. The *Escherichia coli* strain carrying a plasmid with the gene of the α subunit of Qβ replicase was a gift from M. A. Billeter (University of Zurich). Purification of the enzyme was performed as described by Kamen (14) with some changes (G.J.B., unpublished data); the major ones were as follows. Liquid–polymer phase partitioning was done without prior removal of the cell debris by centrifugation. Phosphocellulose was replaced by heparin-Sepharose (Pharmacia) and glycerol gradient centrifugation was replaced by ion-exchange chromatography on DEAE-Sephacel (Pharmacia). After a final concentration step on a small anion-exchanger column packed with Accell-QMA (Waters), fractions were tested for their ability to

The publication costs of this article were defrayed in part by page charge payment. This article must therefore be hereby marked "*advertisement*" in accordance with 18 U.S.C. §1734 solely to indicate this fact.

†To whom reprint requests should be addressed.

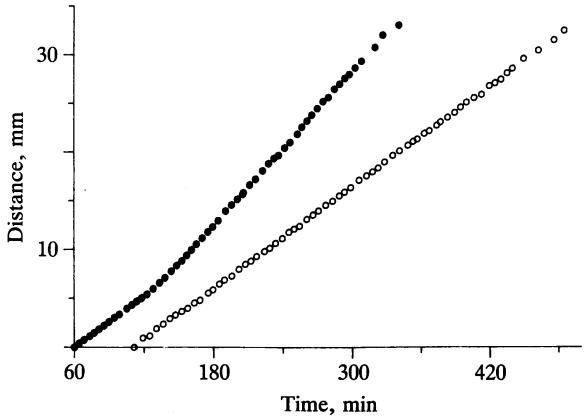

FIG. 1. Experimental concentration wave front vs. time. The position of the MNV_{11} RNA concentration wave front was measured at regular intervals (setup A, laser illumination) over a period of several hours (open circles). In another experiment (solid circles), obtained by inoculating with *de novo* RNA, a sharp change in front velocity occurs at t = 170 min.

perform template-free RNA (*de novo*) synthesis (15). Fractions that showed this ability were used for the following experiments.

Capillary Replication. Precautions against contamination were as described (15). MNV_{11} was provided by C. K. Biebricher (Max-Planck-Institut für Biophysikalische Chemie, Göttingen). Synthesis and separation of the complementary plus and minus strands have been described (16). *De novo* RNA was obtained routinely from tests for template-free purity of the enzyme. The incubation mixture contained 50 mM Tris Cl (pH 7.5), 10% (wt/vol) glycerol, 10 mM $MgCl_2$, 100 mM NaCl, 15 μM ethidium bromide, 10 mM dithiothreitol, 0.5 mM ATP, 0.5 mM CTP, 0.5 mM GTP, 0.5 mM UTP, and 1.8 μM enzyme. A polyethylene tube (1 mm, i.d.) was filled with the incubation mixture, followed at one end by 0.5 μl of a 1 μM solution of one of the above RNA species as indicated below. The replication propagation and monitoring are described below. The tube was then frozen at −70°C, cut into 2.5-mm pieces, and soaked in 20 μl of 50 μM EDTA (pH 8.0). Fractions were stored at −20°C.

Online Detection System. Ethidium bromide has been widely used to determine nucleic acid concentrations (17, 18). The dye intercalates into double-helical nucleic acid regions and in the bound state shows as much as 100 times the fluorescence of the free state. The excitation maxima of the bound dye are red-shifted to 320 nm and 520 nm; the emission maximum remains at 590 nm. Titration curves with the self-replicating RNA molecule MNV_{11} under replication conditions show signal changes in the concentration range from 0.01 to 10 μM (G.J.B., unpublished data).

Two experimental setups were used. In setup A, ethidium bromide fluorescence in the capillary was excited axially at 514 nm by a fiber optic-coupled argon laser. The wave front was measured using a parallel hair pointer mounted on an electronically monitored screw drive, accurate to 0.01 mm. In setup B, parallel observation of capillaries was allowed. Capillaries were mounted on a rectangular holder provided with a length scale, were placed on an ultraviolet transilluminator (366 nm), and were illuminated only when photographs were taken. At regular time intervals the apparatus was photographed using a Polaroid MP camera equipped with a Wratten red 23A gelatin filter and type 55 Polaroid film. The fronts were located by scanning the negatives with a LKB 2222 Ultra-Scan XL laser densitometer. The ambient temperature in setup A was 22°C and in setup B was 30°C.

THE KINETIC MODEL

For a single species of palindromic RNA (the plus and minus strands are then identical), the following three-step replication mechanism has proved consistent with more extensive simulated schemes and with experiments on the homogeneous kinetics (4):

$$I + E \xrightarrow{k_{a3'}} {}_1IE \xrightarrow{k_E} {}_nIE + I$$

$$ {}_nIE \xrightarrow{k_{d5'}} I + E \quad \text{and} \quad I + I \xrightarrow{k_{ds}} I_2, \qquad [3]$$

where I is the information-carrier RNA, ${}_1$IE and ${}_n$IE are the complexes with the enzyme E before and after production and release of the replica, I_2 is the RNA duplex, $k_{a3'}$ is the rate constant for association at the 3′ end, k_E is the rate constant for elongation with release of replica, $k_{d5'}$ is the rate constant for dissociation at the 5′ end, and k_{ds} is the rate constant for double strand formation of RNA.

The reaction–diffusion equations for this scheme then take the form

$$\frac{d[I]}{dt} = D_1\frac{\partial^2[I]}{\partial x^2} - k_{a3'}[E][I] + k_E[{}_1IE] + k_{d5'}[{}_nIE] - k_{ds}[I]^2,$$

$$\frac{d[{}_1IE]}{dt} = D_2\frac{\partial^2[{}_1IE]}{\partial x^2} + k_{a3'}[E][I] - k_E[{}_1IE],$$

and

$$\frac{d[{}_nIE]}{dt} = D_3\frac{\partial^2[{}_nIE]}{\partial x^2} + k_E[{}_1IE] - k_{d5'}[{}_nIE], \qquad [4]$$

with the conservation of enzyme requiring $[E] + [{}_1IE] + [{}_nIE] = [E]_0$ (the initial concentration of enzyme). This is a system of partial differential equations for the three concentrations of I, ${}_1$IE, and ${}_n$IE as a function of the distance x along the capillary and the time t. If all concentrations are expressed in units of μM and time is in minutes, then typical values of the parameters for MNV_{11} in the experiments are $k_E = 1.5$, $k^*_{a3'} = k_{a3'}[E]_0 = 60$, $k_{d5'} = 0.9$, and $k_{ds} = 0.3$.

There are two distinct homogeneous kinetic regimes (4): an exponential growth regime with the rate coefficient κ determined by the leading eigenvalue of the system linearized near $[I] = 0$ ($\kappa \approx \sqrt{k_E k_{d5'}}$ for $k^*_{a3'} >> k_E > K_{d5'}$) and a linear growth phase in which the concentrations of ${}_1$IE, ${}_n$IE, and (depending on the magnitude of k_{ds}) I are constant with growth rate $v \approx \kappa_{lin}[E]_0[\kappa_{lin} \approx k_{d5'}k_E/(k_{d5'} + k_E)]$. Ultimately, the RNA net growth drops to zero as a result of product inhibition and substrate depletion. This is true of the single-strand RNA concentration in the above scheme and so we focus on the concentration of I in the calculations below. The double-strand RNA concentration is not large at the concentration where the front is detected.

EXPERIMENTAL RESULTS

The homogeneous kinetics of MNV-11 replication, under the same conditions as used in the capillary experiments, is shown in Fig. 2. The exponential phase of growth is clearly seen in the logarithmic plot and the linear phase follows. The slope of the logarithmic growth curve is just $f(u)/u$ and it is straightforward to deduce from the experiment that $f'(u)$ (see text after Eq. 1) is a decreasing function of u.

The results of following the front in a typical experiment with MNV-11 are shown in Fig. 1. The points lie on a straight line, indicating a constant front velocity: measurements started after 110 min in this case. The front velocity was maintained for more than 6 hr. The initial decay in the front velocity (data not shown), after inoculation, is characteristic of the establishment of the nonlinear wave (see *Discussion*)

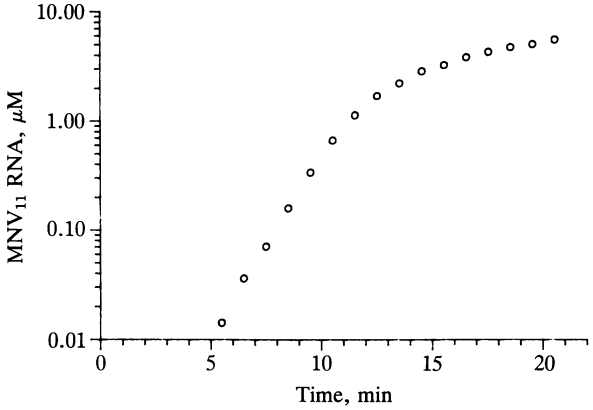

FIG. 2. Homogeneous kinetics of MNV_{11} replication. The capillary-replication incubation mixture was used, but with 0.9 μM enzyme and 0.5 mM [α-^{32}P]ATP (500 Ci/mol; 1 Ci = 37 GBq). The reaction mixture (200 μl) was inoculated with 1 pmol of MNV_{11} minus strands. Replication was started by increasing the temperature from 0°C to 22°C. Aliquots (5 μl) were withdrawn and the reaction was stopped immediately by mixing with 15 μl of loading buffer containing 20 mM EDTA (pH 8.0), 3% (vol/vol) Ficoll, 0.025% bromophenol blue, and 0.025% xylene cyanol in deionized formamide. AMP incorporation was measured as μmol of acid-insoluble [α-^{32}P]AMP per liter. Replication rates were determined as described (19). Two phases can be seen, an exponential phase where the (total) RNA concentration is lower than the enzyme concentration and a linear phase where the RNA concentration is higher than the enzyme concentration (19).

and depends on the detailed technique used for inoculation (initial concentration profile). Occasional impurities could be distinguished from later *de novo* assembly (15) of replicating RNA by the time of appearance and by gel electrophoresis of the extracted portion. In several experiments, we observed the early initiation of a pair of fronts and the ultimate collision of two of the traveling waves.

The magnitude of the velocity measured, after the initial relaxation, was 1.447 ± 0.002 μm/sec or 0.0868 mm/min. This velocity varied about 5% between different experiments under identical conditions. The initial velocity, after a first detection of the front, was up to a factor of 4 greater. The homogeneous replication rate constants, measured under identical conditions, were $\kappa = 1.3 \pm 0.1 \times 10^{-2}\ s^{-1}$ in the exponential phase and $\kappa_{lin} = 0.9 \pm 0.2 \times 10^{-2}\ s^{-1}$ in the linear phase. $k^*_{a3'}$ has been estimated to be 60 $\mu M^{-1}\cdot min^{-1}$ (M. Werner, personal communication). Then the formulas for κ and κ_{lin} (4) are easily inverted to give $k_E = 1.48\ min^{-1}$ and $k_{d5'} = 0.86\ min^{-1}$. The observed single-strand RNA saturation concentration may be used to deduce $k_{ds} = 0.34\ \mu M^{-1}\cdot min^{-1}$.

Using the effective Fisher formula, justified below, $v = 2\sqrt{\kappa D}$, allows the diffusion constant to be calculated as $D = 0.40 \pm 0.05 \times 10^{-6}\ cm^2/s$. A calculation of the radius of the RNA–enzyme complex from the Stokes–Einstein relation $D = kT/6\pi\eta R$, with the viscosity η = 1.3 centipoise and temperature 21°C, gives a value of $R = 4.2 \pm 0.6$ nm. This value may be compared with an estimate based on the sedimentation analysis (20) of a globular protein (horse liver catalase; M_r = 221,600) of similar molecular weight to the Qβ holo-enzyme (M_r = 215,000): R = 4.9 nm. By contrast, MNV_{11} has a value of $R \approx 3.1$ nm [cf. tRNA, $D = 0.7 \times 10^{-6}\ cm^2/s$ in water at 20°C (21)]. The experiments favor an interpretation in which the effective diffusion constant is that of the complex (see below).

A sharp change in front velocity is shown in Fig. 1, obtained by using a *de novo* RNA as the inoculum under identical conditions with setup A. Product analysis of the replicating RNA in the course of the traveling wave forms the most direct evidence for selective evolutionary changes. In another experiment, with the MNV_{11} inoculum, the front position was measured using setup B and the products from successive short (2.5 mm) segments along this capillary were analyzed electrophoretically. The results are displayed in Fig. 3. New bands are seen to appear in the course of the experiment and to replace the original ones, with the point of equal concentration occurring where the front velocity changes sharply.

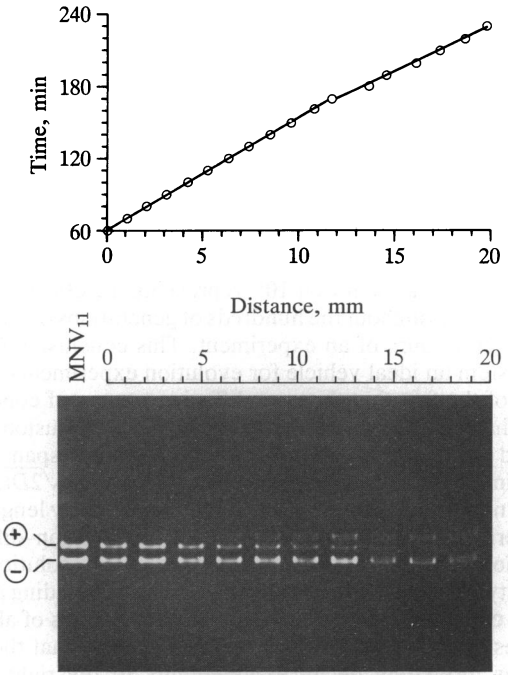

FIG. 3. Evolution of a new quasi-species along the capillary. (*Upper*) Front position measured using setup B. (*Lower*) Gel containing the fractions at 2.5-mm intervals. Regression lines are shown for the periods before and after 170 min. Aliquots (2 μl) of the fractions were withdrawn after 240 min, mixed with 2 μl of loading buffer, boiled for 3 min to melt the double strands, immediately chilled on dry ice, and loaded into the gel slots. The polyacrylamide gel contained 13% (wt/vol) acrylamide and 0.26% *N,N'*-methylenebisacrylamide in running buffer (100 mM Tris borate, pH 8.3). Electrophoresis was for 6 hr at 5 V/cm at 4°C (16). Lane MNV_{11} contains MNV_{11} single strands (plus and minus strands) as reference. The concentration shift to new bands is centered at 12 mm where the velocity changes.

DISCUSSION

Front Velocity and Concentration Profile. Analytical work on the single-component reaction–diffusion equation (1) has exposed the asymptotic approach to a wave traveling with the minimum velocity of Eq. 2 (12, 22–24). An analytic solution for a traveling wave solution to Eq. 1 has been found for a velocity very near to the minimum velocity (25). For a velocity of $v = 5\sqrt{kD/6} \approx 2.04\sqrt{kD}$, the front profile of the traveling wave is

$$u(z) = K\left[1 + \exp\left(z\sqrt{\frac{k}{6D}}\right)\right]^{-2}, \qquad [5]$$

in the variable $z = x - vt$. This demonstrates the exponential decay of the concentration with a decay length $\lambda = \sqrt{3D/2k}$. The asymptotic decay length at the minimum velocity is calculated below as $\sqrt{D/k}$. The slicing of the plastic capillary across the front zone is not yet sufficiently accurate to allow precise measurements on the width of the front. An order of magnitude estimate for the front width may be made based on the observed fluorescence intensity profile:

the front that could be located to within ± 0.1 mm and the visible concentration change in RNA may be estimated from the width of the fluorescence titration curve to be a factor of 10 or so, and so the exponential decay length is ≈0.06 mm. A reduction to single-molecule concentrations then occurs over a distance of ≈1.5 mm. The enzyme concentration of 1.8 μM then corresponds to about 10^{11} RNA molecules in the exponential growth phase at any time, for a capillary with the experimental radius of ≈0.5 mm. As far as evolution experiments are concerned, we conclude from this simple single-component treatment that 10^{11} represents the effective population size throughout the hundreds of generations occurring in the several hours of an experiment. This conclusion renders the system an ideal vehicle for evolution experiments. Use is made of the fact that the pure diffusive erasure of concentration changes is, in contrast to the reaction–diffusion wave, limited to distances of ≈2 mm in the time span of the experiment, the distance scale growing only as $\sqrt{2Dt}$.

We now show how the front velocity and decay length may be derived for the multicomponent replication–diffusion equations (Eq. 4). Consider a traveling wave solution with velocity v and let $z = x - vt$. If we consider the leading portion of the concentration wave, where concentrations of all RNA species are small and further make the ansatz that the three species ultimately decay exponentially to the right of the front, ([I] = $c_1e^{-\lambda z}$, [$_1$IE] = $c_2e^{-\lambda z}$, and [$_n$IE] = $c_3e^{-\lambda z}$), then the reaction–diffusion system (Eq. 4) reduces to the matrix equation

$$\begin{pmatrix} \lambda(D_1\lambda - v) - k^*_{a3'} & k_E & k_{d5'} \\ k^*_{a3'} & \lambda(D_2\lambda - v) - k_E & 0 \\ 0 & k_E & \lambda(D_3\lambda - v) - k_{d5'} \end{pmatrix} \times \begin{pmatrix} c_1 \\ c^2 \\ c_3 \end{pmatrix} = 0. \quad [6]$$

The condition for a nontrivial solution is that the determinant is zero, and a real root λ for which c_1, c_2, and c_3 are positive is required. In the special case where all diffusion constants are equal (value D), the solution may be obtained explicitly from the quadratic $\kappa = \lambda(D\lambda - v)$, where κ is just the homogeneous exponential-phase rate constant. The condition for a real $\lambda > 0$ is that the discriminant $v^2 - 4D\kappa \geq 0$, giving the minimum velocity $v = 2\sqrt{D\kappa}$ when $\lambda = \sqrt{D/\kappa}$. In the general case, the minimum velocity is the smallest $v > 0$ satisfying the above condition.

In the limit of high binding constant of RNA to enzyme ($k^*_{a3'}$ large), a straightforward expansion of Eq. 4, assuming $D_2 = D_3$, shows that the diffusion coefficient is that of the complex and the replication rate just that obtained in the homogeneous kinetics in the same limit. This has been confirmed by direct calculation of the roots λ from Eq. 6 and by a full simulation. The above argument requires that the replication rate coefficient decrease with increasing concentration of RNA: this is demonstrated in the homogeneous kinetic results of Fig. 2. For two other multicomponent systems of reaction–diffusion equations that have been investigated (26, 27), this does not hold.

Selection in RNA Traveling Waves. Figs. 1 and 3 demonstrate that evolution of new RNA species occurs in the course of the experiments. Since the replication at any point occurs for a significant time in the linear phase of growth, where selection pressures can be different from those in the exponential phase (6) (e.g., allowing coexistence), we investigated numerically the competition in the capillary between MNV_{11} and a variant assigned parameters to give it an advantage only

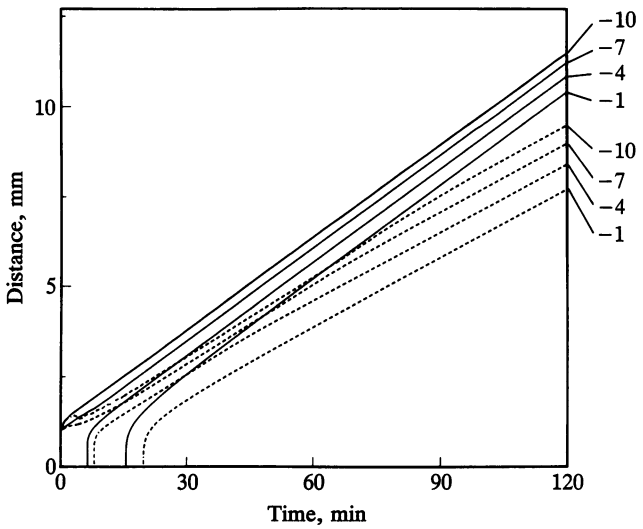

FIG. 4. Selection by wave front separation. Calculated contours (labeled in powers of 10) for the concentrations of two RNA species (in μM): one with the kinetic parameters of the variant used in the experiments and the other replicating faster in the linear phase ($k_{a3'} \times 4$, $k_E/2$). The calculation uses a six-component-coupled reaction–diffusion discretization, coupled through the common enzyme replicase. The dashed contours belong to the variant faster in the linear phase and the solid contours to the variant faster in the exponential phase. Note the separation of the wave fronts and the slowing of the second (dashed) front, indicating selection.

in the linear phase ($k^*_{a3'} = 240\ \mu M^{-1}\cdot min^{-1}$, $k_{d5'} = 0.43\ min^{-1}$ with the other parameters as in *Results*). The six-component system of equations was discretized by standard techniques (28) with a fixed regular spatial grid of as many as 800 points. Replication was cut off at a lower concentration corresponding to the presence of just a single molecule in the volume at the front in which exponential growth takes place ($V \approx 1$ μl, cf. the above expression for the front width). Fig. 4 shows contours of constant concentration for the two species as function of space and time. Two fronts emerge traveling at different velocities with MNV_{11} leading with a velocity, $v \approx 0.086$ mm/min (identical with the minimum value of v that yields a positive solution to Eq. 6). The trailing variant invades the linear phase of MNV_{11} growth with a front moving about 30% more slowly. This is sufficient to ensure selection of MNV_{11} over moderate propagation distances through separation of the fronts (invasion once the linear phase is complete is impossible).

We thank S. Völker, M. Schwierzeck, W. Simm and his technicians, G. Goldmann, R. Oberdiek, and M. Meyer for technical assistance; C. Biebricher for helpful discussions pertaining to the homogeneous kinetics; and M. Eigen for providing a constantly favorable environment for this research.

1. Zhabotinsky, A. M. (1967) *Oscillatory Processes in Biological and Chemical Systems* (Science Publ., Moscow), p. 252.
2. Schneider, F. W. (1976) *Biopolymers* **15**, 1–14.
3. Mills, D. R., Peterson, R. I. & Spiegelman, S. (1967) *Proc. Natl. Acad. Sci. USA* **58**, 217–224.
4. Biebricher, C. K., Eigen, M. & Gardiner, W. C., Jr. (1983) *Biochemistry* **22**, 2544–2558.
5. Biebricher, C. K., Eigen, M. & Gardiner, W. C., Jr. (1984) *Biochemistry* **23**, 3186–3194.
6. Biebricher, C. K., Eigen, M. & Gardiner, W. C., Jr. (1985) *Biochemistry* **24**, 6550–6560.
7. Eigen, M. (1971) *Naturwissenschaften* **58**, 465–523.
8. Thompson, C. J. & McBride, J. L. (1974) *Math. Biosci.* **21**, 127–142.
9. McCaskill, J. S. (1984) *J. Chem. Phys.* **80**, 5194–5202.
10. Eigen, M., McCaskill, J. S. & Schuster, P. (1988) *Adv. Chem. Phys.*, in press.
11. Fisher, R. A. (1937) *Ann. Eugen.* **7**, 355–369.

12. Kolmogorov, A., Petrovsky, I. & Piscounov, N. (1937) *Moscow Univ. Bull. Math.* **1**, 1–25.
13. Murray, J. D. (1977) *Lectures on Nonlinear-Differential-Equation Models in Biology* (Clarendon, Oxford), pp. 217–233.
14. Kamen, R. (1972) *Biochim. Biophys. Acta* **262**, 88–100.
15. Sumper, M. & Luce, R. (1975) *Proc. Natl. Acad. Sci. USA* **72**, 162–166.
16. Biebricher, C. K., Diekmann, S. & Luce, R. (1982) *J. Mol. Biol.* **154**, 629–648.
17. Tao, T., Nelson, J. H. & Cantor, C. R. (1970) *Biochemistry* **9**, 3514–3532.
18. Le Pecq, J. B. (1971) *Methods Biochem. Anal.* **20**, 41–86.
19. Biebricher, C. K., Eigen, M. & Luce, R. (1981) *J. Mol. Biol.* **148**, 391–410.
20. Sober, H. A., ed. (1970) *Handbook of Biochemistry* (Chemical Rubber, Cleveland), p. C-11.
21. Olson, T., Fournier, M. J., Lankgley, K. H. & Ford, N. C., Jr. (1976) *J. Mol. Biol.* **102**, 193–203.
22. Fife, P. C. (1979) *Lecture Notes in Biomathematics* (Springer, Berlin), Vol. 28.
23. Rothe, F. (1984) *Lecture Notes in Mathematics* (Springer, Berlin), Vol. 1072.
24. Mimura, M. (1982) *Lecture Notes in Biomathematics* (Springer, Berlin), Vol. 54.
25. Ablowitz, M. J. & Zeppetella, A. (1979) *Bull. Math. Biol.* **41**, 835–840.
26. Dunbar, S. (1983) *J. Math. Biol.* **17**, 11–32.
27. Aoki, K. (1987) *J. Math. Biol.* **25**, 453–464.
28. Smith, G. D. (1985) *Numerical Solution of Partial Differential Equations* (Clarendon, Oxford), 3rd Ed.